Diffusion in a Slightly Ionized Gas with Application to Effusion from a Shock Tube

BRADFORD STURTEVANT
Guggenheim Aeronautical Laboratory, California Institute of Technology, Pasadena, California
(Received February 13, 1961)

A sampling technique for measuring the diffusive flux of charged particles from an ionized gas to a cold wall by measuring the effusive electrical current through a small orifice in the wall has been used to study slightly ionized argon behind reflected shock waves. The technique is described and the transient diffusion process upon which it depends is considered in some detail. Computations based on a simple one-dimensional isothermal charge diffusion model illustrate the features and give the result that the effect of the electric body forces is generally greater on the ions and less on the electrons than originally expected. These results are used in an approximation to the nonisothermal problem to give a relation between the measured effusive current and the ion density in the hot gas. Preliminary observations of the dependence of ion density on time and temperature in the initial stages of ionization relaxation are reported. Simple considerations of the chemical kinetics indicate that for the portion of the process observed (degree of ionization about 10^{-5} times the equilibrium value) the ionization of argon results from a complicated series of consecutive reactions.

I. INTRODUCTION

A MOLECULAR beam type of sampling device which utilizes the effusion of charge particles from a shock-heated gas has been used to study the ionization process in the region between the end wall of a shock tube and the reflected shock wave.[1] Electrons and ions formed by the ionizing reactions diffuse through the growing thermal layer adjacent to the cold end wall (Fig. 1) and effuse through a small orfice in the wall to a highly evacuated chamber. The instantaneous flux of either electrons or ions through the orifice is measured as an electric current by separating them just downstream of the orifice with a transverse electric field and collecting them on electrodes. This current is a very sensitive measure of the degree of ionization in the reflected shock region (typical ionization levels in the experiments reported here are $\alpha \sim 10^{-7}$).

Since the technique involves time-dependent charge transfer to the end wall, it is analogous to the more familiar shock-tube *heat*-transfer technique in which the measured thermal behavior of, e.g., a thin film on the end wall is related to conditions in the gas by a heat-transfer theory. In the present case, if the orifice is sufficiently small that it does not disturb the thermal layer, a "charge-transfer theory" describing the diffusion to the cold end wall relates the measured current to the degree of ionization in the shock-heated gas. It is the purpose of this paper to describe this theory and its application to the experiments. Conditions are such that there are many collisions in the diffusion layer, so only continuum concepts are used in the diffusion theory.

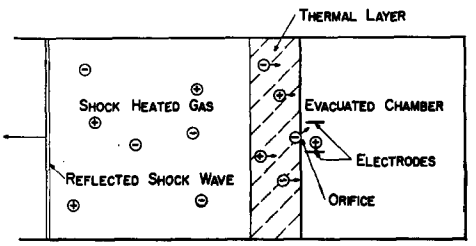

FIG. 1. Schematic drawing of the sampling experiment.

As with heat transfer, the shock-tube end-wall diffusion problem is one of the simplest cases because of its one-dimensionality, the minor role of convective velocities, and the absence of applied fields or wall currents. Therefore many of the features of the general problem of containment of hot ionized gases in cold containers, currently of some interest, appear here in simple form. The property that is of interest in the application of the sampling experiments is the ion flux to the wall, but other features such as the particle distributions throughout the layer, the behavior of the electric field, and the possibility of a steady-state solution are also of general interest. In the next section some of these properties are outlined analytically and others are exhibited in numerical solutions to the diffusion equations. Comparison is made with the quasi-neutral or "ambipolar diffusion" assumption.

[1] This work was reported in part in B. Sturtevant, "Effusion of charged particles from a shock heated gas," GALCIT Rept. California Institute of Technology, Pasadena, California, 1960 (unpublished).

The motivation for the development of the sampling technique lies in the desire to use shock tubes to study low-density gases. It is evident that the class of molecular-beam techniques which has been so useful in studies of mass spectroscopy, nuclear resonance, etc., may also become very useful in low-density shock-tube studies. The application of the simple end-wall diffusion theory to the present sampling device is restricted to low densities by the requirement that the orifice not disturb the thermal layer, i.e., that the mean free path be larger than the orifice diameter. Typically, shocks at about Mach number 7 running into argon at about 0.1 mm Hg are reflected from the end wall to produce a stagnant body of gas at about 10 000°K and 20 mm Hg. At these conditions the equilibrium degree of ionization is about 1%, but the ionization process is so slow that only its initial stage is observed in the available experimental time of about 20 μsec. The processes that lead to the initial ionization are not understood, although they are felt to involve atom-atom collisions and to be very slow (determining the relaxation time). The experimental results presented in Sec. III confirm the latter point and indicate that an unspecified but complicated set of consecutive reactions results in the production of argon ions.

The *steady-state* effusion of charged particles from a glow discharge has frequently been used as an ion source in mass spectrometry. Recently, sampling techniques have been used to study the details of glow discharges.[2] The theory of ambipolar effusion for glow discharge diagnostics has been worked out in detail by Pahl[3] and applied experimentally by Weimer.[4]

II. CHARGE DIFFUSION

In order to best exhibit the behavior of a slightly ionized gas near a cold wall we consider the simplest time-dependent example which contains all the essentials: one-dimensional isothermal diffusion from the region $x > 0$, in which ionization and recombination are neglected, to a plane metallic wall ($x < 0$) when, initially, the charge number density for $x > 0$ is uniform [$n_i(x, 0) = n_e(x, 0) \equiv n_\infty$] and the electric field is zero [$E(x, 0) = 0$]. Conditions at $x = \infty$ are undisturbed from the initial conditions. The connection between this model and the reflected shock problem is evident and will be discussed at the end of this section. The important facts that the metallic wall acts as a strong sink to electrons and ions and that electric body forces play a dominant role can be incorporated into this model. The possibility that thermal and pressure diffusion may exist and that fluid quantities (e.g., density and therefore diffusion coefficients) may be variable is of secondary importance and is omitted.

Since temperature and gas density are assumed constant and the gas is slightly ionized, the charge diffusion does not affect the neutral gas and vice versa, so we need only consider the *binary* mixture of electrons and ions. The isothermal assumption is furthermore useful because the important subcase of isothermal equilibrium has been extensively studied and serves as an instructive limit.

A well-known feature of mixtures of electrons and ions is that charge neutrality tends to be preserved except near bounding surfaces. The general problem of the behavior of a plasma near a body is, in fact, a boundary-layer problem. Whereas far away from the body (or any discontinuity) the plasma can be considered neutral and the usual equations of magneto-fluid dynamics applied, near the body charge separation is essential to the accurate description of the effect of the wall. This situation is analogous to the classical fluid-mechanical case in which potential flow and slip boundary conditions are sufficient to describe flow "far away" from a body, but boundary-layer theory is required for the description of the flow "near" the body. In the present problem diffusion plays the same role as viscosity does in the classical boundary layer.

Von Laue, Schottky, and others pioneered the theoretical study of the steady-state case (isothermal equilibrium) in the early part of the century[5] and showed the boundary-layer behavior. This layer became known as the "sheath" and was often treated as a discrete layer of finite thickness which patched the outer flow to physically realistic boundary conditions.[6] This patching is particularly straightforward conceptually when the mean free path is larger than the Debye length (the "free fall sheath"), but in general leads to difficulty if more than a crude description is desired. Langmuir introduced further sublayers to fill in the details.

The physics can be represented accurately by

[2] Cf., for example, R. L. F. Boyd and D. Morris, Proc. Phys. Soc. (London) **68**, 1 (1955).
[3] M. Pahl, Z. Naturforsch. **12a**, 632 (1957).
[4] U. Weimer, Z. Naturforsch. **13a**, 278 (1958).
[5] This work is reviewed with references in R. H. Fowler, *Statistical Mechanics* (The University Press, Cambridge, England, 1955), Chap. 11; cf. also F. H. Clauser, "Plasma dynamics," Johns Hopkins University, Department of Aeronautics, AFOSR TR-59-125 (1959).
[6] Cf., for example, I. Langmuir, Phys. Rev. **43**, 224–251 (1933).

accounting for charge diffusion in an "inner solution" which is matched to the outer solution with the boundary condition at $x = \infty$ as in boundary-layer theory. We study here the case equivalent to the flat-plate boundary layer in which the outer "flow" (at $x = \infty$) is undisturbed.

Boundary Conditions at the Wall

One of the most difficult aspects of the general diffusion problem is the boundary condition at the wall-gas interface, particularly the electric boundary conditions and the effect of recombination at the wall. The electric fields in the gas generally induce electric fields (and therefore polarization, etc.) in the wall and the electric boundary condition consists of an appropriate matching of these responses. The electrostatic response of a metallic wall is particularly simple because of the mobility of its conduction electrons. Charge is induced in sheets on the surface (as, e.g., with condenser plates) giving a jump in field from zero within the metal to $E(0, t)$ at the surface. This field is then matched to the field in the gas at $x = 0$. From charge conservation, the charge at the surface is equal and opposite to the net charge in the gas, so the electric jump $E(0, t)$ results from the net loss of charge from the gas to the wall by diffusion.

Depending on the initial conditions and on the wall temperature, two different charge sheet configurations are possible: In the case of a "cold wall," the thermionic electron emission from the wall is less than the initial electron flux at the wall, $\frac{1}{4}n_\infty \bar{c}_e$, where $\bar{c}_e$ is the electron mean thermal velocity at $x = \infty$, and a net positive charge builds up in the gas with an equal and opposite negative charge at the surface. This is the case to be considered in this paper and is distinguished by the fact that there is always an abundance of electrons at $x = 0$ available for recombination. On the other hand, with a "hot wall" there is initially a net flux of electrons into the gas and a resultant positive sheet at the surface which presumably may consist either of fixed metal ions or adsorbed gas ions.

For isothermal equilibrium (i.e., no reaction) the particle density boundary condition results simply from the thermodynamic requirement that the chemical potential be continuous at the interface. For example, in the case of an electron atmosphere bounded by a metallic wall, the chemical potential of the electrons in the metal involves the work function, and the matching amounts to equating the effusive flux from the gas to the thermionic emission from the metal. This simple condition is not directly applicable to the present time-dependent (nonequilibrium) problem except for large time when as shown below, the *electrons* are approximately in isothermal equilibrium. The emission of electrons from the cold wall is generally extremely small so the nearly equal and opposite effusion from the gas is necessarily small, i.e., $n_e(0, t) \ll n_\infty$.[7] It is concluded that a good approximation is $n_e(0, t) = 0$.

The recombination reaction at $x = 0$ is catalyzed by the wall which acts as a massive third body. The electron sheet at the surface of a "cold wall" is analogous to the adsorbed layer of reactant in ordinary molecular surface catalysis. In this case the "adsorption" forces are related to the image forces that act on charged particles near conducting surfaces (that is, Coulomb forces rather than van der Waals or chemical forces as in the usual case), but the details of the process are not understood. As a result, the recombination reaction and therefore the particle density boundary conditions cannot be described quantitatively. The reaction rate depends in general on the surface concentrations (number per unit area) of the reactants and on the properties of the wall material. The concentration of electrons is extremely high and, due to the high mobility of metal electrons, the rate constant must be very high. Therefore, for reasonable reaction rates, the ion surface concentration must be very small. Correspondingly, the volume ion density $n_i(0, t)$ is also probably small; $n_i(0, t) \doteq 0$.

Diffusion Equations

The equations describing a general electron-ion boundary-layer problem are derivable from the conservation equations for fluid flow (including electromagnetic body forces), Maxwell's equations, and associated relations such as the equation of state and the relations between forces and fluxes (e.g., thermal gradients and heat flux). For the simple problem considered here the equations reduce to the two continuity equations for electrons and ions, the mass flux-force relations, and Maxwell's equations. Furthermore, due to the one-dimensionality and initially zero magnetic field, Maxwell's equations reduce to the Poisson equation (mks units)

$$\partial E/\partial x = (e/\epsilon_0)(n_i - n_e), \tag{1}$$

where E is the electric field, e the electronic charge, and ϵ_0 the dielectric constant of vacuum.

[7] One argument involving photoemission leads to $n_e(0, t)/n_\infty \sim 10^{-16}$ for a representative case; interpretation of the shorting of thin-film heat-transfer gauges with the theory of this section leads to an experimental value $n_e(0, t)/n_\infty \sim 10^{-15}$ (reference 1, pp. 76 and 108).

The continuity equations are

$$(\partial n_e/\partial t) + (\partial F_e/\partial x) = 0, \tag{2}$$

$$(\partial n_i/\partial t) + (\partial F_i/\partial x) = 0, \tag{3}$$

where $F_{e,i}$ is the number flux per unit area and time. The flux-force relations express the assumed linearity between mass transfer and concentration gradients or body forces,

$$F_e = -D_e\left(\frac{\partial n_e}{\partial x} - \frac{e}{kT}n_eE\right), \tag{4}$$

$$F_i = -D_i\left(\frac{\partial n_i}{\partial x} + \frac{e}{kT}n_iE\right), \tag{5}$$

where $D_{e,i}$ is the diffusion coefficient and k the Boltzmann constant.

Defining the nondimensional quantities $x' = x/\lambda$ where $\lambda = (\epsilon_0 kT/e^2n_\infty)^{\frac{1}{2}}$ is the Debye length, $t' = t/\tau$, where $\tau = \lambda^2/D_e$, $N = n_i/n_\infty$, $n = n_e/n_\infty$, $F' = F\lambda/n_\infty D_e$, $E' = eE\lambda/kT$ and $D = D_i/D_e = (m_e/m_i)^{\frac{1}{2}}$, a small parameter, and combining Eqs. (2) and (3) with (4) and (5), gives

$$N_{t'} = D[N_{x'x'} - (NE')_{x'}], \tag{6}$$

$$n_{t'} = n_{x'x'} + (nE')_{x'}, \tag{7}$$

$$E'_{x'} = N - n \tag{8}$$

with initial conditions $n(x', 0) = N(x', 0) = 1$, $E(x', 0) = 0$ and boundary conditions $N(0, t') = n(0, t') = 0, N(\infty, t') = n(\infty, t') = 1, E(\infty, t') = 0$. The subscripts indicate differentiation. Nondimensionalizing Eqs. (4) and (5) and combining Eqs. (1), (2), and (3) gives the following useful auxiliary relations:

$$F'_i = -D(N_{x'} + NE'), \tag{9}$$

$$F'_e = -n_{x'} + nE', \tag{10}$$

$$E'_{t'} = F'_e - F'_i. \tag{11}$$

Equations (6) and (7) are diffusion-type equations which are coupled by the nonlinear electric body force terms. Due to the nonlinearity the equations cannot be solved in closed form. The small parameter D, 0.0037 for argon, expresses the slowness of ion diffusion compared to electron diffusion. It appears in Eq. (6) in such a way that the ion diffusion is a singular perturbation of a "frozen ion" solution (N = const). Consequently an "inner" ion diffusion and "outer" electron diffusion configuration is indicated. One composite expansion in D which can be set up for the complete solution unfortunately results in the zeroth-order approximation [Eqs. (6), (7), and (8) with $D = 0$] remaining nonlinear, although all higher approximations are linear.

A crude way of visualizing the process for small time, when E' and $E'_{x'}$ are small, is to neglect the coupling terms in Eqs. (6) and (7) ("free diffusion"). This leads to

$$N = \operatorname{erf}[x'/2(Dt')^{\frac{1}{2}}], \tag{12}$$

$$n = \operatorname{erf}[x'/2(t')^{\frac{1}{2}}], \tag{13}$$

$$E' = 2(Dt')^{\frac{1}{2}}\operatorname{ierfc}\frac{x'}{2(Dt')^{\frac{1}{2}}} - 2(t')^{\frac{1}{2}}\operatorname{ierfc}\frac{x'}{2(t')^{\frac{1}{2}}}, \tag{14}$$

where erf ξ is the error function,

$$\operatorname{erf}\xi = \frac{2}{(\pi)^{\frac{1}{2}}}\int_0^\xi \exp(-\eta^2)\,d\eta,$$

and ierfc ξ is the integral of the complementary error function,

$$\operatorname{ierfc}\xi = \int_\xi^\infty (1 - \operatorname{erf}\eta)\,d\eta.$$

Note that electron diffusion is the major feature for small time.

On the other hand, the scale difference between electron and ion diffusion does not appear in the steady-state problem ($N_{t'} = n_{t'} = 0$). It is evident, then, that the nature of the diffusion process must change somewhere between $t' = 0$ and $t' = \infty$. If a potential $V' = eV/kT$ is defined by $V'_{x'} = -E'$ and $V'(\infty, t) = 0$, then Eqs. (6) and (7) can be integrated at $t' = \infty$ to give $N = e^{-V'}$ and $n = e^{V'}$, the Boltzmann distribution for *isothermal equilibrium*. Note that if $n(0) < 1$, then $N(0) > 1$. However, for a cold wall we know that $n(0)$ and $N(0) < 1$, so there is no steady-state solution to the problem as posed. A well-known property of the steady state is that the effect of the wall extends about one Debye length into the gas.

The characteristic time τ is the time for an electron to diffuse one Debye length and for the experiments reported below is typically 10^{-9} sec near the wall. The diffusion at large time can be studied by stretching the time coordinate with D,

$$t_1 \equiv Dt' \tag{15}$$

so that the characteristic time is $\tau/D = \lambda^2/D_i \sim 10^{-6}$ sec. The equations then become

$$N_{t_1} = N_{x'x'} - (NE')_{x'}, \tag{16}$$

$$Dn_{t_1} = n_{x'x'} + (nE')_{x'}, \tag{17}$$

$$E_{x'} = N - n. \tag{18}$$

There is no longer a singular perturbation and because of the coupling terms the electron and ion diffusion have the same scale. The effect of the electric field has been to slow down electron diffusion and speed up ion diffusion.

To a first approximation ($D = 0$), Eq. (17) gives $n(x', t') = e^{V'(x', t')}$: The electrons are locally in isothermal equilibrium. That is, they adjust instantaneously to any changes in field resulting from ion diffusion.

Ambipolar Diffusion

A common approximation to Eqs. (6), (7), and (8) which expresses this result is the assumption of quasi-neutrality or ambipolar diffusion, $n = N$. Eqs. (6) and (7) then determine the problem

$$n_{t'} = [2\ D/(1 + D)]n_{x'x'}, \tag{19}$$

$$E' = [(1 - D)/(1 + D)](n_{x'}/n), \tag{20}$$

while Eq. (8) serves as a check on the approximation. The solution to Eqs. (19) and (20) with boundary conditions [Eq. (8)ff] is

$$N = n = \operatorname{erf} \frac{x'}{2\{[2\ D/(1 + D)]t'\}^{\frac{1}{2}}}, \tag{21}$$

$$E' = -\frac{1 - D}{[2\pi\ D(1 + D)t]^{\frac{1}{2}}} \exp - \frac{x'^2}{[8\ D/(1 + D)]t} \cdot \left(\operatorname{erf} \frac{x'}{2\{[2\ D/(1 + D)]t'\}^{\frac{1}{2}}}\right)^{-1}. \tag{22}$$

Numerical Solution

The exact solution to Eqs. (6), (7), and (8) has been obtained numerically on the Burrough's 220 digital computer at the Caltech Computing Center. The results exhibit the details of the processes discussed qualitatively above and are compared here

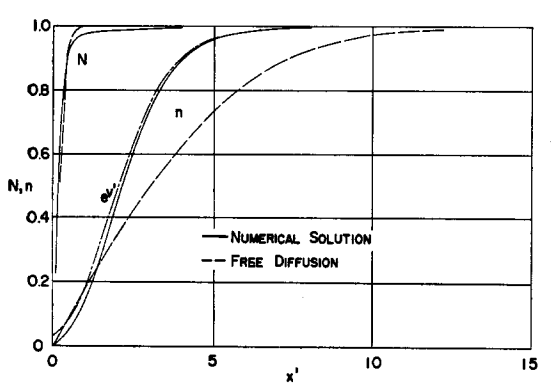

FIG. 2. Electron and ion profiles at $t' = 10$.

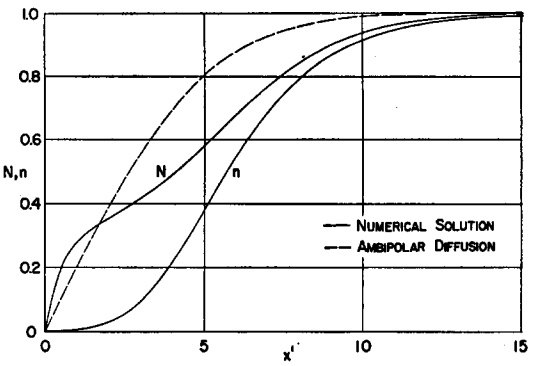

FIG. 3. Electron and ion profiles at $t' = 1000$.

with the free diffusion and ambipolar diffusion results [Eqs. (12), (13), (14) and (21), (22)].

At the suggest of Dr. J. N. Franklin of the Computing Center, the Crank-Nicholson method[8] for numerical analysis of initial value problems was used on Eqs. (6) and (7), iterating around values of E' obtained from Eq. (8) using the trapezoidal rule. K. J. Herbert wrote the program and supervised the computation. The calculation proceeded from $t' = 0.002$ through six decades to $t' = 1000$. The x' domain and mesh size were changed at each half-decade by trial and error to accommodate the growth of the diffusion layer and minimize computing time insofar as stability allowed. It was sufficient to use about 80 x' points and 40 t' steps per half-decade until instabilities required 100 time steps for $100 < t' < 300$ and 350 steps for $300 < t' < 1000$. The total computing time is about $2\frac{1}{2}$ hr of which the last hour is for $300 < t' < 1000$.

Typical electron and ion distributions appear in Figs. 2 and 3. No significant departure from free diffusion appears until $t' = 1$, when features appear that are characteristic for all later time: The gross effect of the field is to slow down electron diffusion and thereby make the profile fuller. However, from Eq. (10) and the boundary conditions, the flux to the wall is given by $F'_e(0, t') = -n_{x'}(0, t')$, so for slower diffusion the slope near the wall must be less and the profile shallower. These two requirements combine to give a distribution with an inflection point. For the ions the effect is opposite and no inflection point is required. However, it turns out that the ions eventually diffuse so fast (much faster than predicted by ambipolar diffusion) that a profile with *two* inflections develops!

It can be seen in Fig. 2 that by $t' = 10$ the electron density differs from the Boltzmann distribution by

[8] R. D. Richtmyer, *Difference Methods for Initial Value Problems* (Interscience Publishers, Inc., New York, 1957), p. 93.

only a few percent. By $t' = 100$ it agrees to better than one percent.

Figure 4 illustrates the behavior of the electrical field E' with time. The field at the wall reaches a minimum of -2.51 at $t' = 60$ (corresponding to a field of -43 v/cm for a typical example of the present experiments). It is evident that eventually E' decreases to arbitrarily small values everywhere. This result is completely hidden in the "ambipolar diffusion" approximation, (Eq. 22), where, for example, $E'(0, t') = -\infty$. It appears from extrapolation that the electric field disturbance propagates *30 Debye lengths* into the gas before its absolute value decreases everywhere below say 0.1. On the other hand, the potential $V'(0, t')$ at the wall continues to grow negatively at least until $t' = 1000$, attaining a value of -6.7 (a voltage of -0.23 v for a gas at room temperature).

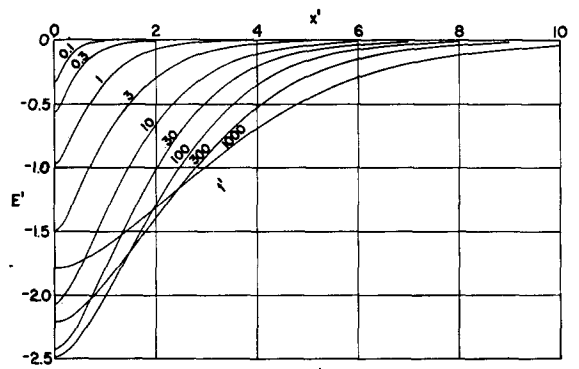

FIG. 4. Electric field profiles.

Figure 5 summarizes the characteristics of the particle distributions far away from the the wall by exhibiting the growth of the electron and ion boundary layers, $\delta_{e,i}(t')$ is the distance from the wall at which the particle density reaches 0.09. At $t' = 1000$, the layer thickness seems to be approaching a $t^{\frac{1}{2}}$ behavior with an absolute value just twice that for free ion diffusion.

A plot of the particle fluxes to the wall (Fig. 6) characterizes the diffusion near the wall. The crossover at $t' = 60$ was entirely unexpected and is one of the more interesting manifestations of the electric body force exhibited by the exact solutions. The electron flux approaches the value predicted by ambipolar diffusion to within several percent by $t' = 1000$ and apparently the ion flux is also approaching that limit but much more slowly. This is the first feature of the diffusion process for which the ambipolar diffusion result has given a good approximation even if only for very large time.

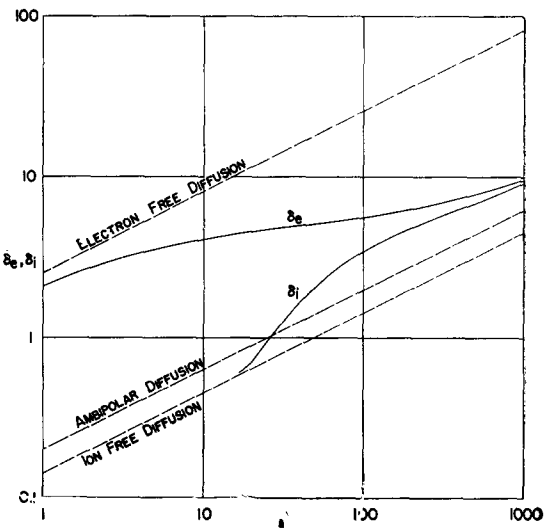

FIG. 5. Electron and ion boundary-layer thickness.

Application to the Sampling Experiments

In order to apply the above theory to the experiments described in Sec. I, one must consider the fact that strong thermal and density gradients exist adjacent to the end wall after shock reflection. As stated above, the presence of a slight degree of ionization does not affect the thermal and dynamic behavior of the neutral gas, so the usual results for the constant-pressure thermal layer[9] apply. Since the thermal diffusion coefficient is generally small and the thermal gradients encountered are no larger than the concentration gradients, thermal diffusion

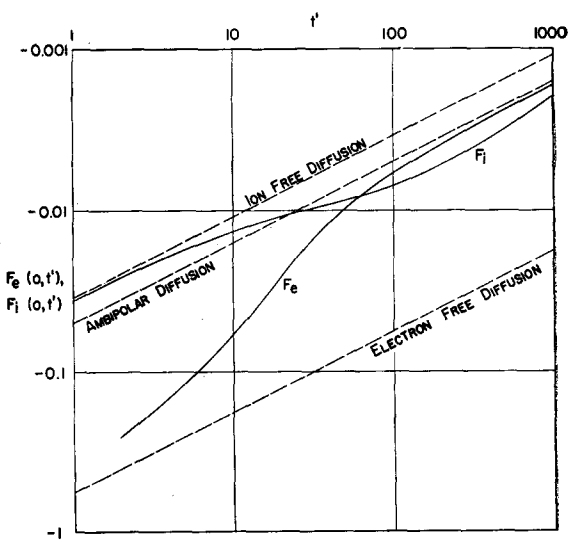

FIG. 6. Flux to the wall.

[9] For example, A. Roshko, "Heat transfer at the end wall of a shock tube" (unpublished), based on the technique of M. D. Van Dyke, Z. angew. Math. u. Phys. **3**, 343 (1952).

is negligible and the only effect of the thermal layer is to make the $D_{e,i}$ in Eqs. (4) and (5) variable. This is analogous to the effect of compressibility encountered in classical boundary-layer theory and one way of accounting for such a variation is to simply use some reference density and temperature in the incompressible solution. We are primarily interested in wall fluxes so the relevant temperature is the wall temperature. This is a particularly convenient approximation since the diffusion coefficients at room temperature are well known.

It is concluded from Fig. 6 that for $t' > 1000$ ($t \gtrsim 3$ μsec for the present experiments) the dimensional flux $F_i(0, t)$ is very nearly $F_i(0, t) = 1.8n_\infty(D_{iw}/\pi t)^{\frac{1}{2}}$ where D_{iw} is evaluated at the wall temperature and reflected shock pressure. In the present experiments the charge density far from the wall is a function of time due to ionization relaxation, $n_\infty = n_\infty(t)$. However, it follows from the boundary-layer-like similarity evidenced by the diffusion process at large time that the functional behavior of $F_i(0, t)$ must be the same, only the constant being changed;

$$F_i(0, t) = -\text{const}\, n_\infty(t)(D_{iw}/t)^{\frac{1}{2}}. \tag{23}$$

Now, if the hole in the end wall is sufficiently small that the diffusion layer is undisturbed (i.e., $\Lambda > d$, where Λ is the mean free path and d is the hole diameter), the particle flux through unit area of hole is given by Eq. (23). In the experiments the hole diameter was 0.32 mm while Λ was typically 0.4 mm in the shock-heated gas and 0.003 mm near the wall. Evidently, the internal part of the layer is affected by the presence of the hole and an additional Reynolds number dependence might appear in Eq. (23). This effect, probably moderate, is neglected here.

A process not discussed above is electron-ion recombination in the cool, dense thermal layer which acts as an additional sink of the diffusing particles. An estimate of its effect can be made by comparing the volume recombination rate near the wall [$(\partial n/\partial t)_R \sim K_R n_\infty^2$, where K_R, the recombination coefficient, is evaluated at wall conditions] with the particle density rate of increase due to the relaxation process,

$$\frac{(\partial n/\partial t)_R}{\partial n_\infty/\partial t} \sim K_R n_\infty t. \tag{24}$$

For a typical experiment with initial pressure = 60 μ Hg, $n_\infty = 3 \times 10^{15}$, $K_R = 3 \times 10^{-13}$ and $t = 2 \times 10^{-5}$, so the recombination effect is less than 1%. However, at higher pressures the effect is larger and is, in fact, observable (see section on experimental results).

III. INCIPIENT IONIZATION IN ARGON

In their investigation of the relaxation time for the ionization of argon, Petschek and Byron[10] concluded that the atom-atom reaction that must account for the initial production of electrons is affected by the presence of small traces of impurities and is sufficiently rate-determining that, in turn, the relaxation time is influenced by impurities. This conclusion was based on the observation of the total radiation emitted from the shocked gas and therefore is open to the question of the contribution of impurity lines. However, the effect has also been observed qualitatively by Alpher and White[11] in interferometric studies. It has become of some interest, therefore, to make a direct study of the initial stages and determine the nature of reactions involved. The experiments reported here represent a preliminary investigation using the sampling technique treated above.

The kinetics of the initial stages is simplified by the fact that the concentrations of the original components, say A and I (e.g., argon and an impurity), remain constant. As a result, a brief consideration of the type of reaction expected is possible and gives a rough idea of functional behaviors: It is thought that a series of consecutive second order reactions in which the products (say 1, 2, etc.) react with A or I (but not with each other, due to the low concentrations in the initial stages) accounts for the eventual ionization of argon. The last of these reactions would be the reaction of ionization products (i.e., electrons) with A or I and is the dominant reaction in the approach to equilibrium. The initial stages are defined as the part of the process in which only forward-going atom-atom reactions are important, a condition which is thought to prevail in the present experiments.

Since only one of the products can play a role in a given reaction, the reactions can be represented schematically as follows;

$$\begin{gathered} A + (A \text{ or } I) \xrightarrow{k_1} 1, \\ (A \text{ or } I) + 1 \xrightarrow{k_2} 2, \text{ etc.} \end{gathered} \tag{25}$$

The rate equations are,

$$\begin{aligned} dn_1/dt &= k_1 n_A n_{A \text{ or } I}, \\ dn_2/dt &= k_2 n_{A \text{ or } I} n_1, \text{ etc.} \end{aligned} \tag{26}$$

[10] H. Petschek and S. Byron, Ann. Phys. (N. Y.) 1, 270 (1957).
[11] R. A. Alpher and D. R. White, Phys. Fluids 2, 162 (1959).

which, since n_A and n_I = const, can be integrated and combined to give

$$n_j = \frac{1}{j!} k_1 k_2 \cdots k_j n_A^{j+1-p} n_I^p t^j, \qquad (27)$$

in which j is the total number of reactions and p is the number of reactions in which I plays a role.[12]

The proportionality constants k_j multiply and, since they contain the usual Boltzmann factors in temperature, the activation energies add. Thus, to ionize one argon atom by any number of reactions requires 15.8-v energy. Combining Eqs. (27) and (23) and using the fact that D_{iw} = const/n_{Aw} = const/$n_{A\infty}T_\infty$ gives the dependence of the ion flux on the ionization reactions,

$$-F_i = \text{const}\ k_1 k_2 \cdots k_j T^{-\frac{1}{2}} n_A^{j+\frac{1}{2}-p} n_I^p t^{j-\frac{1}{2}}, \qquad (28)$$

where the subscript ∞ has been dropped.

The product $k_1 k_2 \cdots k_j$ also contains a pre-exponential temperature factor which for small ranges of temperature can be represented for convenience as a power r of temperature so that $k_1 k_2 \cdots k_j$ = const T^{-r} exp $(-E_+/kT)$, where E_+ is the ionization energy. Therefore

$$\partial \ln F_i/\partial(1/kT) = -E_+ + (r + \tfrac{1}{2})kT \qquad (29)$$

and

$$\partial \ln F_i/\partial \ln t = j - \tfrac{1}{2}. \qquad (30)$$

Several proposals have been made for the actual reactions which could account for the initial stages of argon ionization. (i) Weymann[13] proposes a two-step argon-argon series involving the excitation of argon to the resonance state and subsequent ionization of the excited atom. He shows that this process is more efficient than a one-step argon ionization or impurity ionization providing the impurity level is not too high. (ii) NO formed from air impurity has been thought to be important because of its low ionization potential. However, the total energy required to form NO^+ from free N_2 and O_2 is about 11 v per particle and therefore does not give much of an increase in Eq. (27) over argon ionization unless impurity levels are very high ($\gtrsim$ 1%). In fact, in the present experiments the introduction of air impurity had no noticeable effect until a quenching resulted from the weaker shocks produced in an air-argon mixture for a given diaphragm pressure ratio. (iii) Charge exchange from impurity ions to argon atoms has been mentioned but as shown above would still involve an excitation energy of 15.8 v in the initial stages.

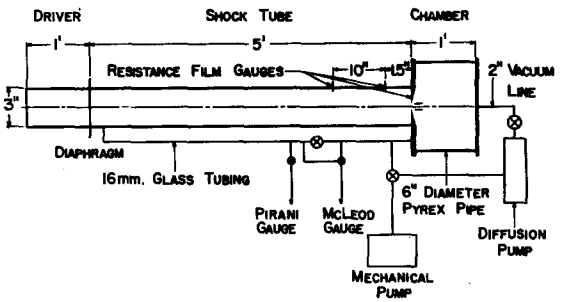

FIG. 7. Schematic diagram of the shock tube.

Experimental Apparatus

The apparatus for the preliminary experiments (Fig. 7) was designed primarily as a vacuum system at the expense of other factors important to shock-tube performance. Simple clamping of the driver to the shock tube provided for quick diaphragm changes so that the system was exposed to atmospheric air for less than $\frac{1}{2}$ min between runs. Otherwise, the tube was kept evacuated at all times. The leak rate was about 5 μ Hg per hour. For a typical run at p_1 = 0.1 mm Hg this resulted in an estimated impurity level of no more than 0.04 %.

Due to the fact that the shock tube was operated at low pressures, its performance was nonideal in two respects. Despite the fact that the tube was 20 diameters long, the shock was still accelerating at the end of the tube. For shock waves at M = 6 and p_1 = 0.1 mm Hg, the speed change was about 4% per foot. (On the other hand, shock waves at p_1 = 10 mm Hg showed little or no acceleration in this tube.) In the present experiments one is concerned with the nonuniformities of temperature and density in the sampling region near the end wall resulting from this acceleration. Since the extent of the sampling region is given by the thermal layer thickness (Fig. 5; for a typical experiment $\delta \sim \frac{1}{2}$ cm), the amount of shock acceleration over this distance and the resulting nonuniformities are negligible. The decrease in shock wave-contact surface separation caused by the loss of gas to the boundary layer in low-pressure shock tubes[14] is evidenced at the end wall by an early arrival of the wave re-reflected from the approaching contact surface. As the pressure level is decreased the

[12] The depletion, $-k_{j+1}n_{A \text{ or } I}n_j$, in the jth reaction is neglected; i.e., it is thought that for the present experiment, not only $n_j/n_{A \text{ or } I} \ll 1$, but that also $k_{j+1}n_j/k_j n_{j-1} \ll 1$.

[13] H. D. Weymann, University of Maryland Institute for Fluid Dynamics and Applied Mathematics, TN BN-144 (1958).

[14] A. Roshko, Phys. Fluids **3**, 835 (1960).

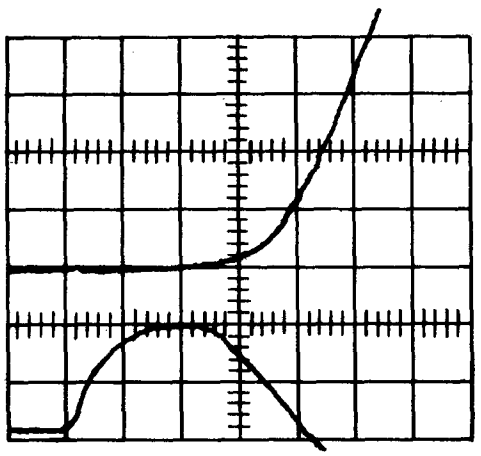

FIG. 8. Typical ion current (upper trace) and end-wall heat-gauge (lower trace) outputs. Time scale 5 μsec/cm, ion current 10^{-9} amp/cm, $p_1 = 100\ \mu$ Hg, $M = 6.55$.

"testing time" for an experiment on the end wall is thereby decreased until, in the present case, the time between incident shock reflection and re-reflected wave arrival is only 20–30 μsec for $p_1 = 0.1$ mm.

The size of the step function signals from standard side-wall and end-wall thin-film heat gauges agreed very well with theoretical predictions of heat transfer down to $p_1 = 0.1$ mm and with measurements in other (longer) shock tubes at Galcit. The shock speed was measured in the usual way with the side-wall gauge signals and the arrival of the shock at the end wall was detected by a similar gauge evaporated onto 2-mil Scotch splicing tape. Complete details of the shock-tube design, calibration, and instrumentation appear elsewhere.[15]

In a typical run the entire system was evacuated to about 10^{-5} mm Hg, flushed with argon, and re-evacuated to the experimental pressure. The valve connecting the tube and chamber (Fig. 7) was closed resulting in further evacuation of the chamber until a pressure ratio of about 500 was set up across the 0.32-mm diameter $\times$ 0.05-mm long hole in the end wall. The mean free path in the chamber was typically about 10 in. The change of pressure in the tube during the few seconds between valve closure and tube firing was negligible. After shock reflection the pressure ratio across the hole was about 10^5.

[15] Reference 1, p. 23.

The electrodes consisted of silver paint painted, baked, and polished on the internal diameter of a piece of 6-mm glass tubing. They subtended a solid angle of 43 deg about the hole center line and were immediately downstream of the hole so that the average particle time of flight to the downstream end of the electrodes was less than 1 μsec. They were biased electrically with respect to the shock tube in such a way (2.6 and -5.4 v) that the electrode currents during a run, as displayed after amplification by a dual-beam scope, were about equal and opposite and unaffected by further increase of bias, indicating that all the electrons were collected by one electrode and all ions by the other.

For obtaining quantitative results the ion current and end wall film gauge outputs were displayed simultaneously (Fig. 8) so that time $t = 0$ could be determined. In Fig. 8 the end wall gauge output shows the familiar shorting effect as the conductivity in the shocked gas becomes significant.

Experimental Results

The ion current at $t = 20$ μsec is plotted in Fig. 9 against the inverse of the reflected shock temperature as computed from the measured Mach number. The decrease of slope with increasing pressure is due to the increasing effect at the high temperature (i.e., high wall densities) of recombination in the thermal layer. Consequently the $p_1 = 60\ \mu$ results are probably the most accurate and will be considered here. The measured logarithmic slope of the best fit dotted line is -12.6, so from Eq. (29), $E_+ = 12.6 + (r + \frac{1}{2})kT$ v. For a many-step process r can be quite large, i.e., 2 or more, so evidently

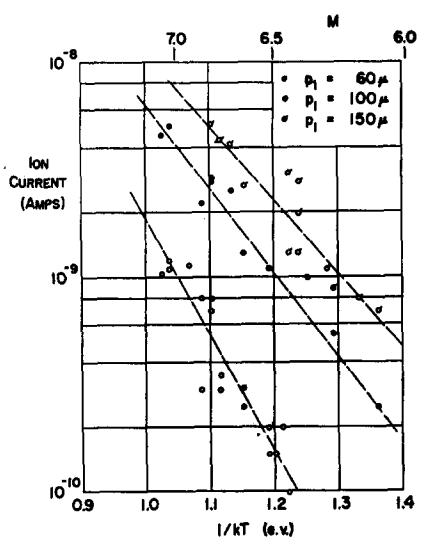

FIG. 9. Ion current at 20 μsec vs 1/kT.

the measured activation energy is quite close to the ionization potential of argon.

A replot on log-log paper of ion current traces from a dozen runs at $p_1 = 60\ \mu$ and Mach numbers 6.4 to 7.1 yields slopes scattering between 5 and 6 around an average of $5\frac{1}{2}$. Therefore, from Eq. (30) $j \sim 6$; a chain of something like *six* consecutive reactions is indicated for the portion of the relaxation process observed.

IV. CONCLUSIONS

The high power-law time dependence, though unexpected, is apparently a quantitative observation of the so-called "incubation time" observed before equilibration in previous experiments. It emphasizes previous observations that the initiation process is slow and therefore has a strong effect on the relaxation time. However, large effects on the charge density were not observed upon introduction of small amounts of impurity (including heated cesium chloride and mercury, and air), i.e., $p \doteq 0$ in Eq. (28). It is concluded that a complicated series of so-far unspecified consecutive reactions results in the ionization of *argon* in the initial stages. It has been demonstrated that sampling techniques have a potential utility in the diagnostics of shock tube and other high-temperature flows. Further experiments for studying ionization relaxation using developments of these techniques are being designed for a new low-density shock-tube facility now under construction at the California Institute of Technology.

ACKNOWLEDGMENTS

The author wishes to express his appreciation to Professors H. W. Liepmann, A. Roshko, and J. D. Cole for their invaluable assistance during the course of this work.

This work was supported by the Office of Naval Research.

THE PHYSICS OF FLUIDS VOLUME 4, NUMBER 9 SEPTEMBER, 1961

Magnetohydrodynamic Results for Highly Dissociated and Ionized Air Plasma

H. T. NAGAMATSU
General Electric Research Laboratory, Schenectady, New York, and Rensselaer Polytechnic Institute, Troy, New York

AND

R. E. SHEER, JR.
General Electric Research Laboratory, Schenectady, New York

(Received January 23, 1961; revised manuscript received May 22, 1961)

An investigation of air plasma moving through a constant (2300 gauss) transverse magnetic field was conducted in a shock tube. As the plasma traveled through the field, an electromotive force was produced in the plasma. Two diametrically opposite, $\frac{1}{2}$-in. diameter, copper electrodes were used to measure this potential. The shock Mach number varied from 10 to 32 with corresponding equilibrium plasma temperatures from 3600° to 11 000°K. At Mach 30 the observed potential across the electrodes, with a 1-meg external load, was 236 v, which agreed with the theoretical value, but at lower Mach numbers the observed potentials were much lower than theory. By varying the external load for a shock Mach number of 30, the current from the plasma varied from nearly zero to 115 amp. This high current was extracted from the copper electrodes at nearly room temperature. The observed potential decreased linearly with increasing current indicating a nearly constant plasma resistance. For this resistance the electrical conductivity was calculated and was much less than the theoretical prediction. The maximum power extracted from the plasma was 7.8 kw with an external load of 1.85 ohms.

I. INTRODUCTION

THERE has been an active interest in recent years by a large number of research workers on the problem of the interaction of plasma with a magnetic field. The need for better understanding of the magnetohydrodynamic phenomena arises from interest in the following areas: thermonuclear reactions, astrophysics, power generation, space propulsion, and application of magnetohydrodynamics to high-altitude hypersonic flight problems. Numerous analytical and only limited experimental papers have been published on the subject.

An investigation was conducted to study the interaction of air plasma, produced by strong shock